The 2025 World Congress on
Advances in Structural Engineering and Mechanics (ASEM25)
BEXCO, Busan, Korea, August 11-14, 2025

Influence of variations in mechanical properties of seismic isolation bearings on the seismic response of a five-span elevated bridge

*Takuma Kubo[1)], Hiroshi Shimmyo[2)]
Shozo Nakamura[3)], Toshihiro Okumatsu[3)], and Takafumi Nishikawa[4)]

[1), 3), 4)] *Nagasaki University, Nagasaki, Japan*
[2)]*Kawakin Core-Tech Co., Ltd. Saitama, Japan*
[1)] bb54125202@ms.nagasaki-u.ac.jp

ABSTRACT

The dynamic verification of bridges utilizing seismic isolation rubber bearings generally employs a bilinear (BL) model for the restoring force in Japan. However, the actual behavior of the products deviates from the BL model due to the Mullins effect and hardening. To address these discrepancies, the tri-linear double target model has been proposed. However, the impact of variations in the properties of the products on bridge response has not been thoroughly investigated. This study established the probability distribution of parameters representing hysteretic properties based on product performance test results and conducted a dynamic analysis using Monte Carlo Simulation. Consequently, the stochastic influence of variations in the properties of the bearings on the seismic response of a five-span elevated bridge was demonstrated.

1. INTRODUCTION

Based on the damage experience of road bridges caused by the 1995 Hyogo-ken Nanbu Earthquake, seismic isolation rubber bearings have been widely introduced as a method to improve seismic performance. Seismic isolation rubber bearings are an effective system to lengthen the natural period of the superstructure and reduce inertial forces. However, the seismic performance of a bridge depends on the energy absorption capacity of the bearings, and their restoring force characteristics significantly influence the seismic behavior of the bridge. Therefore, the restoring force characteristics must be properly modeled in the dynamic analysis of bridges with seismic isolation rubber bearings. In addition, the influence of variations in the mechanical properties (i.e., hysteretic properties) of the bearings on the seismic response of bridges should be considered.

[1)] Graduate Student
[2)] Engineer, Ph.D.
[3)] Professor
[4)] Associate Professor

In actual products, the restoring force characteristics during the first step of loading differ from those in subsequent loading cycles due to their dependency on the maximum loading experienced, which is called the Mullins effect, and hardening occurs even in the allowable displacement range. In the current Specifications for Highway Bridges, V Seismic Design (Japan Road Association 2017), the dynamic verification of bridges utilizing seismic isolation rubber bearings generally employs a bilinear (BL) model to represent the restoring force characteristics. However, it does not consider the Mullins effect and hardening, as illustrated in Fig. 1. To incorporate these effects, the tri-linear double target (DT) model illustrated in Fig. 2 was proposed by Naito et al. (2017). Shimmyo et al. (2021) investigated the influence of the Mullins effect and hardening on the seismic response of a bridge using the DT model. However, the influence of variations in the mechanical properties of seismic isolation rubber bearings on seismic response has not been sufficiently investigated using the DT model. Moreover, in the current design, these variations in the actual products are not considered.

In this context, this study establishes the probability distribution of parameters of the DT model representing the properties based on product performance test results and conducts a dynamic analysis using Monte Carlo Simulation to demonstrate the stochastic influence of variations in the properties of seismic isolation rubber bearings on the seismic response of a five-span elevated bridge.

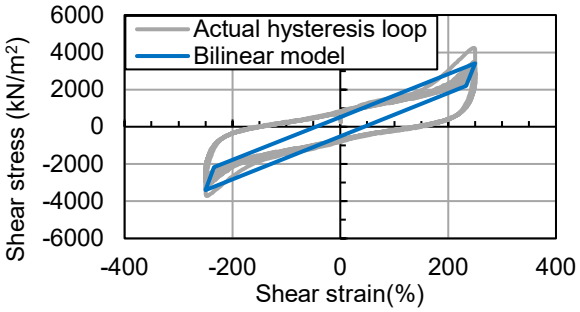

Fig. 1 Comparison between actual hysteresis loop and bilinear model

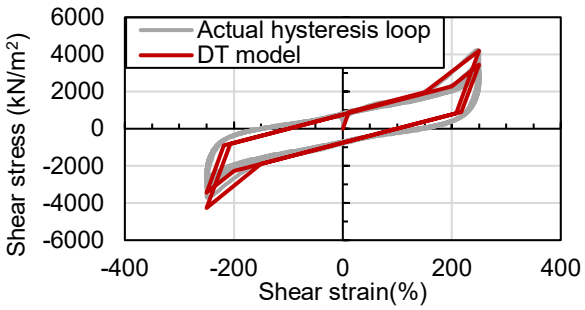

Fig. 2 Comparison between actual hysteresis loop and DT model

2. PARAMETERS OF DT MODEL

Parameters of the DT model are illustrated in Fig. 3 and listed below.

G_1: Skeleton curve secondary stiffness (kN/m^2) for the 1st loop
G_2: Skeleton curve secondary stiffness (kN/m^2) for the 2nd and subsequent loops
G_3: Skeleton curve hardening stiffness (kN/m^2) for the 1st loop
G_4: Skeleton curve hardening stiffness (kN/m^2) for the 2nd and subsequent loops
G_5: Unloading stiffness (kN/m^2)
τ_1: Skeleton curve y-axis intercept stress (kN/m^2) for the 1st loop
τ_2: Skeleton curve y-axis intercept stress (kN/m^2) for the 2nd and subsequent loops
γ_1: Skeleton curve hardening strain (%) ±150% for the 1st loop

γ_2: Skeleton curve hardening strain (%) ±200% for the 2nd and subsequent loops

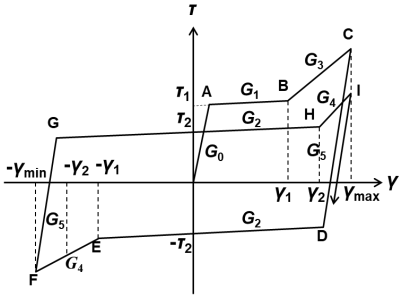

Fig. 3 DT model

These were calculated based on the actual hysteresis loop obtained from the product performance test results, with the exception of G_5. G_5 was set as the equivalent value of the first stiffness of the BL model determined according to the Handbook for Highway Bridge Bearings (Japan Road Association 2019). The shear modulus of the products was 1.2×10^3 (kN/m^2) which was used to determine the first stiffness of the BL model.

τ_1, τ_2, G_1, G_2, G_3, and G_4 were set as variation parameters, considering variations in the mechanical properties, such as the Mullins effect and hardening. τ_1 and τ_2 were calculated by dividing the y-axis intercept forces in the first and second loading loops, respectively by effective shear cross-sectional area. The y-axis intercept forces were set based on the intercept of the actual hysteresis loop obtained from the product performance test results for each Limit State, including Limit States 1 (effective shear strain of 175%), 2 (effective shear strain of 250%) and 3 (effective shear strain of 300%) of the laminated rubber bearing, according to JRA (2019). G_1-G_4 were calculated using the slope of the straight line between each pair of points, including points A to I shown in Fig.3, after determining the coordinates of points A to B on the actual hysteresis loop in Limit States 2 and 3.

3. PROBABILITY DISTRIBUTION OF HYSTERESIS PARAMETERS

3.1 Number of products for evaluating probability distribution

The product performance test data of 128 lead-plugged laminated rubber bearings (LRB) and 118 high-damping laminated rubber bearings (HDR) were used to determine the variation parameters of the DT model. Table 1 lists the number of products used to evaluate the probability distribution.

Table 1 Number of products

Limit state	Effective shear strain	LRB	HDR
	%	Qty. n	
1	175	108	103
2	250	10	8
3	300	10	7
Total		128	118

3.2 Variations in the mechanical properties

Table 2 lists the mean (μ) and standard deviation (σ) for each variation parameter calculated from the product performance test results for all Limit States.

Table 2 Mean and standard deviation of the variation parameters

Type of bearing	statistic	τ_1(kN/m^2)	τ_2(kN/m^2)	G_1(kN/m^2)	G_2(kN/m^2)	G_3(kN/m^2)	G_4(kN/m^2)
LRB	μ	973.0	876.6	770.9	693.4	1914.7	1814.9
	σ	147.5	128.2	98.4	96.1	274.8	365.7
HDR	μ	817.0	655.3	706.3	743.4	2128.0	2009.6
	σ	166.4	115.1	119.0	97.6	424.7	428.3

3.3 Evaluation of probability distributions

Probability distributions were evaluated using both qualitative and quantitative approaches.

First, the estimation was conducted using Kernel Density Estimation (KDE), which is a non-parametric method for qualitatively evaluating similarity to normal distributions. The shape of the sample distributions of each variation parameter, which were expressed as continuous probability distributions using KDE, was compared to the shape of normal distributions composed using the mean and standard deviation of the sample. Fig. 4 shows a comparison of the distribution curve of τ_1 in the LRB.

Next, a quantitative evaluation of the similarity to normal distributions was conducted using a normal Q-Q plot, which is a probability paper. The coefficient of determination (R^2) of the best-fit line was then calculated from the normal Q-Q plot. Fig. 5 shows the normal Q-Q plots of τ_1 in the LRB.

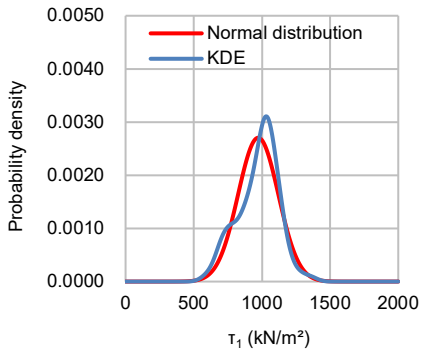

Fig. 4 LRB τ_1 KDE

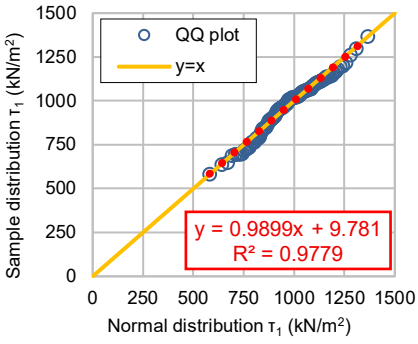

Fig. 5 LRB τ_1 normal Q-Q plot

As shown in Fig. 4, the shape of a sample distribution has approximately the same location of protrusion and spread as the normal distribution. In Fig. 5, the best-fit line coincides approximately with the line given by y=x. Also, R^2 exceeded 0.9. Similar results were obtained for all variation parameters in both LRB and HDR.

Consequently, normal distributions were assumed for all variation parameters.

3.4 The random number data

Random number data were composed from the product performance test results for Limit States 1 and 2. Limit state 3 was eliminated to follow the same calculation conditions in a previous study (Shimmyo 2021). Table 3 shows the number of products used to generate random number data.

Outliers that did not properly reflect the Mullins effect and hardening were eliminated from the sample data before the mean values and standard deviations used for generating random numbers were determined. Values that did not satisfy the following conditions were considered outliers.

1. The intercept stress ratio τ_1/τ_2 was equal to or larger than 1.0, indicating that the intercept stress in the first loop was higher than that in the second loop due to the Mullins effect.
2. The stiffness ratios G_3/G_1 and G_4/G_2 were equal to or larger than 1.0, indicating an increase in stiffness due to hardening.

The mean value and standard deviation of each variation parameter used to generate random numbers are listed in Table 4. Based on the assumption that all variation parameters follow a normal distribution, normal random number data for the dynamic analysis were generated using these values.

Table 3 Number of products for generating random number data

Limit state	Effective shear strain	LRB	HDR
		Qty.	
	%	n	
1	175	105	103
2	250	10	8
Total		115	111

Table 4 Mean and standard deviation for generating random number data

Type of bearing	statistic	τ_1(kN/m^2)	τ_2(kN/m^2)	G_1(kN/m^2)	G_2(kN/m^2)	G_3(kN/m^2)	G_4(kN/m^2)
LRB	μ	974.4	870.5	829.7	762.2	2013.7	2068.7
	σ	144.5	122.5	83.2	73.4	278.0	303.3
HDR	μ	828.3	658.2	752.7	781.8	2269.6	2267.2
	σ	158.8	110.7	105.8	87.3	233.6	293.3

When a normal random number is generated, its value can either be extremely small or large, which is impossible in reality. To address this concern, the range of the normal random number was set as shown in Table 5. The upper and lower bounds were determined based on the maximum value of the differences from the mean value among the minimum value, maximum value of the samples, and the 95% confidence interval.

Table 5 Lower and upper bounds of each variation parameter

(a) LRB

	Lower bound (kN/m^2)	Upper bound (kN/m^2)
τ_1	550.1	1398.8
τ_2	533.0	1208.0
G_1	666.6	992.8
G_2	618.3	906.1
G_3	1468.9	2558.5
G_4	1472.5	2664.9

(b) HDR

	Lower bound (kN/m^2)	Upper bound (kN/m^2)
τ_1	355.6	1301.1
τ_2	347.1	969.3
G_1	545.3	960.1
G_2	610.6	952.9
G_3	1811.8	2727.4
G_4	1692.3	2842.1

Based on the correlation analysis results, a strong correlation was observed between the intercept stresses τ_1 and τ_2. Therefore, regression equations were introduced for τ_1 and τ_2 for both LRB and HDR. Accordingly, the random number data for τ_2 were calculated from the normal random numbers of τ_1 using the regression equation. The regression equations for LRB and HDR are shown in Eqs. (1) and (2), respectively.

It was assumed that all variation parameters, except the intercept stress τ_2, were statistically independent. For each variation parameter, 1000 random numbers were generated to create 1000 DT models.

$$\text{LRB}: \tau_2 = 0.795\tau_1 + 95.49 \quad (1)$$

$$\text{HDR}: \tau_2 = 0.658\tau_1 + 113.13 \quad (2)$$

4. DYNAMIC ANALYSIS

4.1 Analysis structure model

The target bridge shown in Fig. 6 is a five-span continuous plate girder bridge redesigned as a seismically isolated bridge. This target bridge was set referring to the “Dynamic seismic design example of single- and medium-sized reinforced concrete piers” (Public Works Research Center 2006). The target structure for the dynamic analysis is P1 pier of the target bridge. Fig. 7 shows the side view of the single-column RC pier (P1) and the analysis model of P1 on the left and right sides, respectively. All the other parts, except for the plastic hinge of the RC pier, were modeled as linear elements. This pier was designed such that the average shear strain response of the seismic isolation rubber bearing to three level 2 Type II ground motions was

approximately 250% when the hysteresis model of the seismic isolation rubber bearing was the BL model of JRA (2019). Two types of hysteresis models of seismic isolation rubber bearings, BL and DT, were employed.

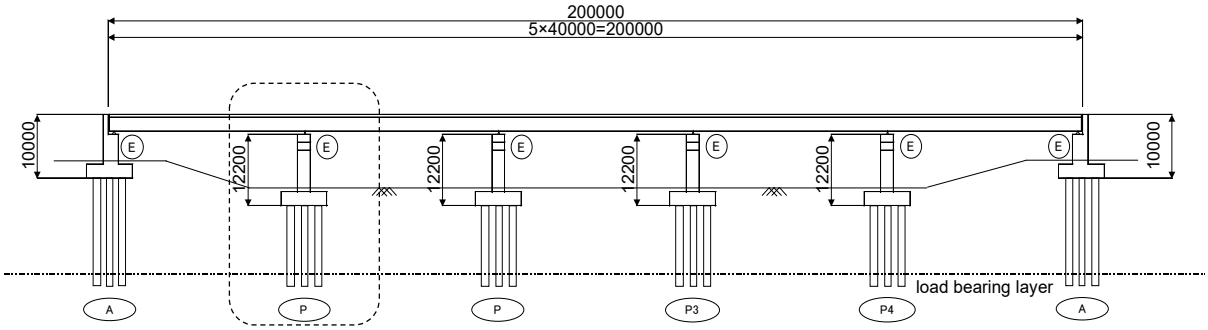

Fig. 6 Target bridge

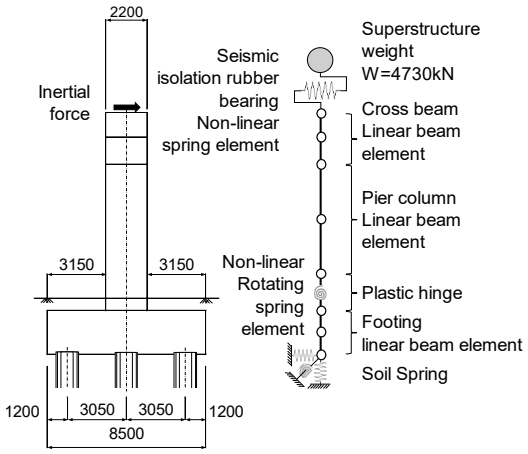

Fig. 7 Side view and analysis model of the RC pier

4.2 Analysis conditions

This dynamic analysis is based on the Specifications for Highway Bridges, V Seismic Design (JRA 2017). The analysis was performed using TDAPIII (ARK Information Systems, Inc. 2019), a three-dimensional dynamic analysis software.

First, eigenvalue analyses were performed for LRB and HDR. Rayleigh damping was determined based on the results of the eigenvalue analysis, and was set for all members except the bearings. Only the hysteresis damping was considered for the bearings.

In the time-history response analysis, the Newmark β method was used as the integration method. The β-value and time interval were set to 0.25 and 0.0020 s,

respectively. Three type II ground motions in Level 2 ground motions for type II ground were used. The ground motions were applied parallel to the bridge axis. The BL model was set based on JRA (2019). The DT models were constructed using 1000 sets of random numbers.

5. SEISMIC RESPONSES

5.1 Histogram of seismic responses

The shear strain and reaction force of the seismic isolation rubber bearings and the rotation angle and bending moment of the plastic hinge on the pier obtained from the dynamic analysis were evaluated. In addition, these responses were averaged over three waves and a histogram was created for each response in the DT model. The results of the BL model as design values were overlaid on the histograms for comparison. Based on this comparison, the probability of exceeding the design value Pr[Ex.d]) was calculated. Moreover, the probability of exceeding the limit value Pr[Ex.l] was calculated for the shear strain of the bearing and rotation angle of the plastic hinge. The limit values of the shear strain were set to 250% for Limit State 2 and 300% for Limit State 3 based on JRA (2019). The limit value of the rotation angle of the plastic hinge corresponding to Limit State 2 was set based on the Design Guidelines for Highway Bridges, Part II: Bridge Construction (Nippon Expressway Research Institute Company Limited 2015). Fig. 8 and 9 show histograms of the seismic responses for the LRB and HDR, respectively.

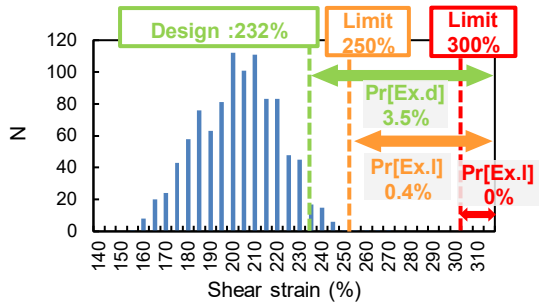

(a) Shear strain

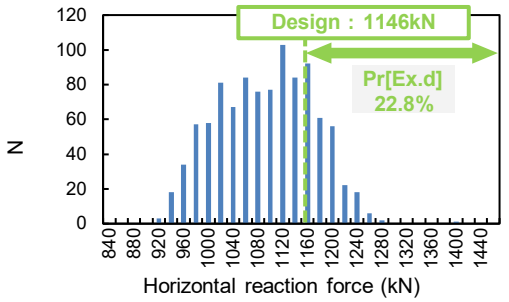

(b) Horizontal reaction force

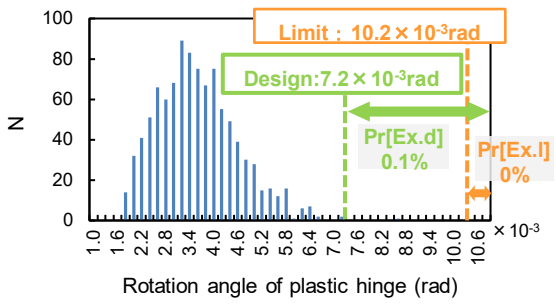

(c) Rotation angle of plastic hinge

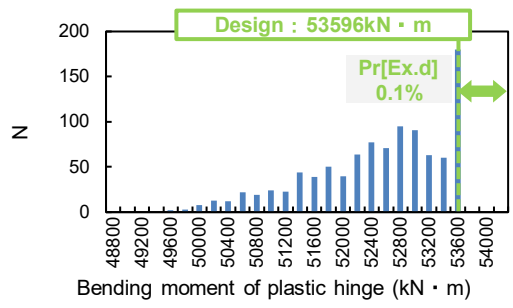

(d) Bending moment of plastic hinge

Fig. 8 LRB histograms of seismic responses

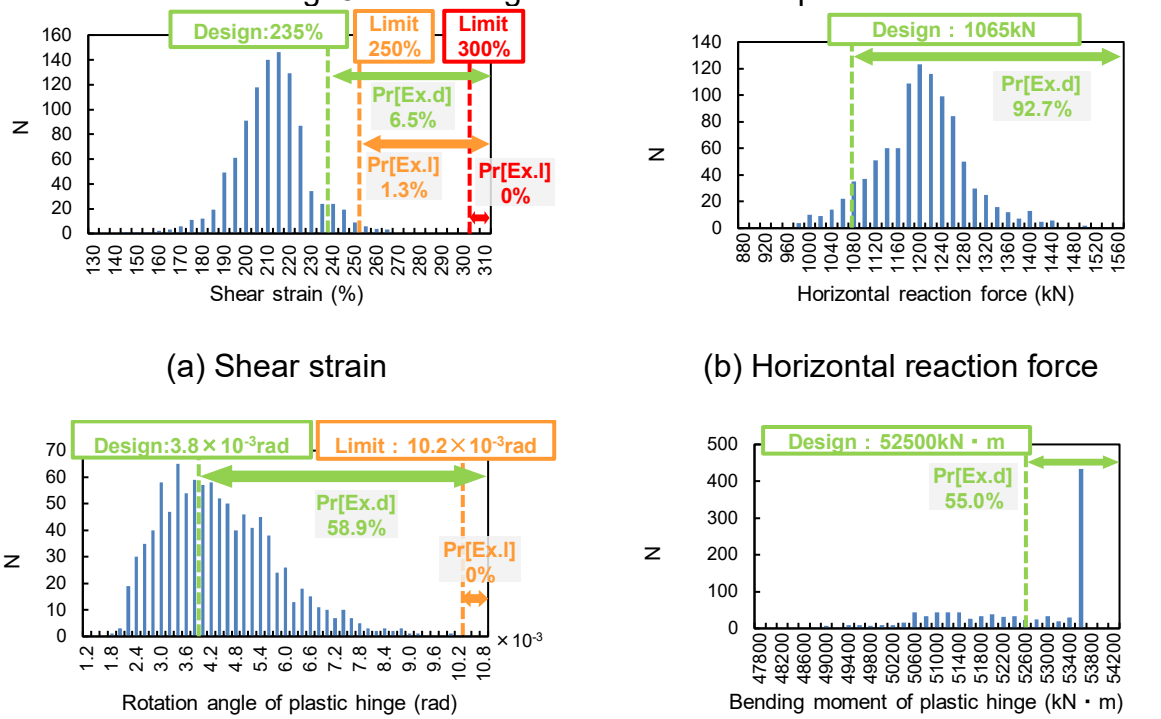

(a) Shear strain

(b) Horizontal reaction force

(c) Rotation angle of plastic hinge

(d) Bending moment of plastic hinge

Fig. 9 HDR histograms of seismic responses

Figs. 8 and 9 demonstrate that variations in the mechanical properties have a minor influence on the shear strain of the bearing. However, these variations have a relatively large influence on the horizontal reaction force of the bearing. The observed difference in the influence of the variations may be caused by the occurrence of hardening. In the case of the LRB, the influence of the variations on the pier response was minimal. However, in the case of the HDR, the variations have a relatively large impact on the pier response. This result suggests that, in the case of LRB, the exceedance of pier responses over the design values due to an increase in the bearing reaction force caused by hardening could be suppressed by the energy absorption capacity of the bearings. Furthermore, in the case of HDR, Pr[Ex.d] was higher than that of LRB for all response parameters.

According to Figs. (a) and (c) in Figs. 8 and 9, the Pr[Ex.I] values are relatively low. However, if the design values are closer to the limit values under different conditions, the safety of the bearing and pier responses may be lost due to the influence of the variations.

5.2 Comparison of the hysteresis area

Differences were observed in the probability of exceeding the design value for each bearing type. These differences were investigated by focusing on the hysteresis

area for the mean models shown in Fig. 10, where the BL and DT models are indicated by the blue and red lines, respectively.

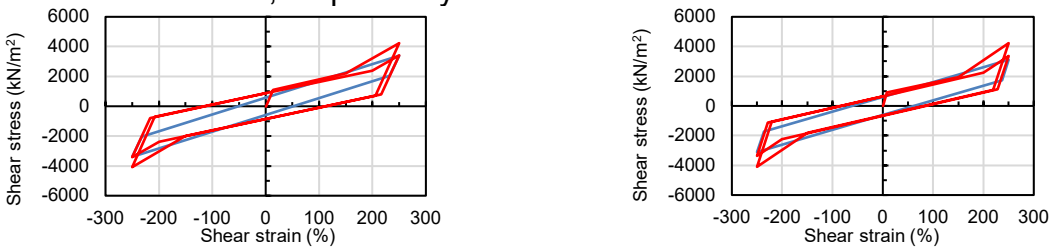

(a) LRB Mean model (b) HDR Mean model

Fig. 10 Comparison of the hysteresis area

Fig. 10 shows that the hysteresis area of the DT model is smaller for the HDR than for the LRB. Since the hysteresis area represents the energy absorption capacity, the smaller the hysteresis area, the larger the bearing and pier responses. Therefore, it is believed that the Pr[Ex.d] of the HDR was higher than that of the LRB. Moreover, in the HDR, there is concern that the Pr[Ex.d] of pier responses is relatively high since there were few cases in which the energy absorption capacity of the DT model was larger than that of the BL model.

6. CONCLUSIONS

The main findings of this study are summarized as follows.

(1) Focusing on the Pr[Ex.d] of the bearing responses, it was found that the variations in the mechanical properties of the bearings have a small impact on the shear strain of the bearings, whereas they have a relatively large impact on the reaction forces of the bearings for both the LRB and HDR.
(2) Focusing on the Pr[Ex.d] of pier responses, it was found that the variations in the mechanical properties of bearings have a small impact on the rotation angle and the bending moment of the plastic hinge for the LRB, whereas they have a relatively large impact on the pier responses for the HDR.
(3) All Pr[Ex.I] were sufficiently low. However, if the design values are closer to the limit values under different conditions, the safety of the bearing and pier responses may be lost due to the variations in the mechanical properties of the bearings.
(4) In general, the HDR has a stronger tendency than the LRB for the hysteresis area of the DT model to be smaller than that of the BL model.

The following issues need to be addressed in future studies.

(1) It is necessary to correct more product performance test results to improve the accuracy of examinations.
(2) Similar studies should be conducted under different design conditions and bridge types to obtain more general conclusions.
(3) It is necessary to determine the number of simulations required to obtain reliable results.

(4) It is necessary to revise dimensions if the pier and the bearing in the target structure to evaluate safety more accurately.

REFERENCES

ARK Information Systems, Inc (2019), TDAPIII Batch Version User's Guide.

Japan Road Association (2017), Specifications for Highway Bridges, V Seismic Design.

Japan Road Association (2019), Handbook for Highway Bridge Bearings.

Naito, N., Mazda, T., Uno, H. and Kawakami, M. (2017), "Seismic performance evaluation of LRB considering Mullins effect and hardening", J. JSCE, Ser. A1, **73**(4), I_499-I_510 (in Japanese).

Nippon Expressway Research Institute Company Limited (2015), Design Guidelines for Highway Bridges, Part II: Bridge Construction published.

Public Works Research Center (2006), Dynamic Seismic Design Method Manual for Bridges.

Shimmyo, H., Onal, T., Nakamura, S., Tokunaga, K. (2021), "Influence of Mullins and hardening effects of seismic isolation rubber bearings on the seismic response", IABSE Congress, Ghent 2021, Structural Engineering for Future Societal Needs, 1444-1452.